

# $\pi$ -Extended Ladder-Type Conjugated Polymers via BN-Annulation

Peirong Qiang<sup>#a</sup>   
 Zuobang Sun<sup>#a</sup>   
 Bai Xue<sup>\*a</sup>   
 Fan Zhang<sup>\*a</sup> 

<sup>a</sup> School of Chemistry and Chemical Engineering, State Key Laboratory of Metal Matrix Composites, Shanghai Jiao Tong University, Shanghai 200240, P. R. China  
 fan-zhang@sjtu.edu.cn; bxue79@sjtu.edu.cn

<sup>#</sup> Equally contributed.

Dedicated to Professor Peter Bäuerle on the occasion of his 65th birthday.

Received: 17.01.2021  
 Accepted after revision: 01.03.2021  
 DOI: 10.1055/s-0041-1727181; Art ID: om-21-0011oa

License terms: 

© 2021. The Author(s). This is an open access article published by Thieme under the terms of the Creative Commons Attribution-NonDerivative-NonCommercial License, permitting copying and reproduction so long as the original work is given appropriate credit. Contents may not be used for commercial purposes, or adapted, remixed, transformed or built upon. (<https://creativecommons.org/licenses/by-nc-nd/4.0/>)

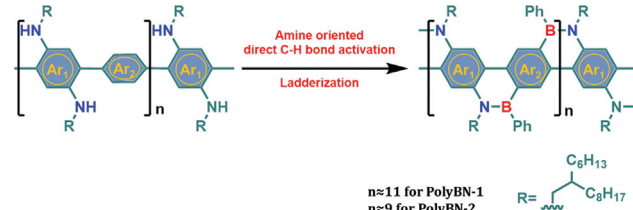
**Abstract** Two kinds of ladder-type conjugated polymers were concisely synthesized by the formation of single-stranded conjugated polymers via Stille cross-couplings, followed by nitrogen-directed electrophilic borylations at electron-rich aromatic rings. The resulting BN-annulated polymers show good film-forming behaviors and high air and thermal stability. Their structurally shape-persistent rigid backbones render them with  $\pi$ -extended conjugation, allowing for efficient light harvesting in the low-energy regions, and emitting strong fluorescence with narrow emission widths.

**Key words** ladder-type polymers, BN-annulation,  $\pi$ -extended conjugation, light harvesting, fluorescence emission

## Introduction

Distinctly different from the conventional conjugated polymers, ladder conjugated polymers (cLPs) possess fully fused backbones comprising multiple strands of covalent bonds, which restrict the freely torsional motion between adjacent aromatic rings.<sup>1–3</sup> Thanks to the rigid coplanar skeletons, cLPs always exhibit excellent thermal stability,  $\pi$ -extended conjugation, and also tend to generate strong intermolecular  $\pi$ - $\pi$  stacking interactions in some cases, thus favorable for  $\pi$ -electron delocalization, long-range exciton diffusion, and fast intra-chain charge/phonon transport in comparison with those single-bond-linked conjugated polymers.<sup>4–11</sup> Accordingly, these intrinsic characters make such kinds of polymers arousing tremendous attention over a quite broad range, such as nonlinear optics, organic light emitting diodes, organic field effect transistors and photovoltaics.<sup>12–19</sup>

However, searching for an efficient ladderization reaction to concisely construct a new type of fully conjugated



polymer with promising properties is still full of challenge. Conventionally, in order to achieve a ladder polymer, the two strands of covalent bonds could be constructed simultaneously upon a one-step reaction performance, such as the Diels–Alder reaction.<sup>20–25</sup> However, in another stepwise performance, a single-stranded polymeric structure could be formed at first, which was further annulated into the ladder structure by the formation of the second strand of bonds. Given that such a stepwise synthetic strategy could be established on the basis of versatile available either synthetic reactions or monomers, thus it has become an efficient tool for the construction of various cLPs.<sup>26–35</sup> Recently, several groups including ourselves have successfully synthesized some ladder-type boron (B) and nitrogen (N)-containing heteroacenes in excellent isolated yields, dominantly attributing that Lewis acidic boron atoms enable smoothly conducting condensation with a Lewis base amino group, and strong electrophilic attack on aromatic rings. The incorporation of such BN units with C = C isoelectronic structure into these heteroacenes can generate the similar geometric structures to their full carbon analogues, but significantly different electronic structures and self-assembly behaviors. Undoubtedly, such kinds of heteroacenes considerably expanded the molecular regimes of organic semiconducting materials with huge potential applications in high-performance electronic devices.<sup>36–46</sup> Unfortunately, as far as we know, BN-embedded polymers are still rarely explored, likely due to the lack of available monomers. We have successfully synthesized the C<sub>2h</sub>-symmetric BN-heteroacenes via a 2-fold successive electrophilic borylation (Figure 1),<sup>39</sup>

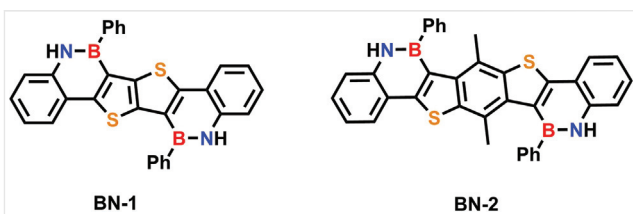


**Figure 1** The structures of ladder-type BN-embedded heteroacenes termed BN-1 and BN-2.<sup>39</sup>

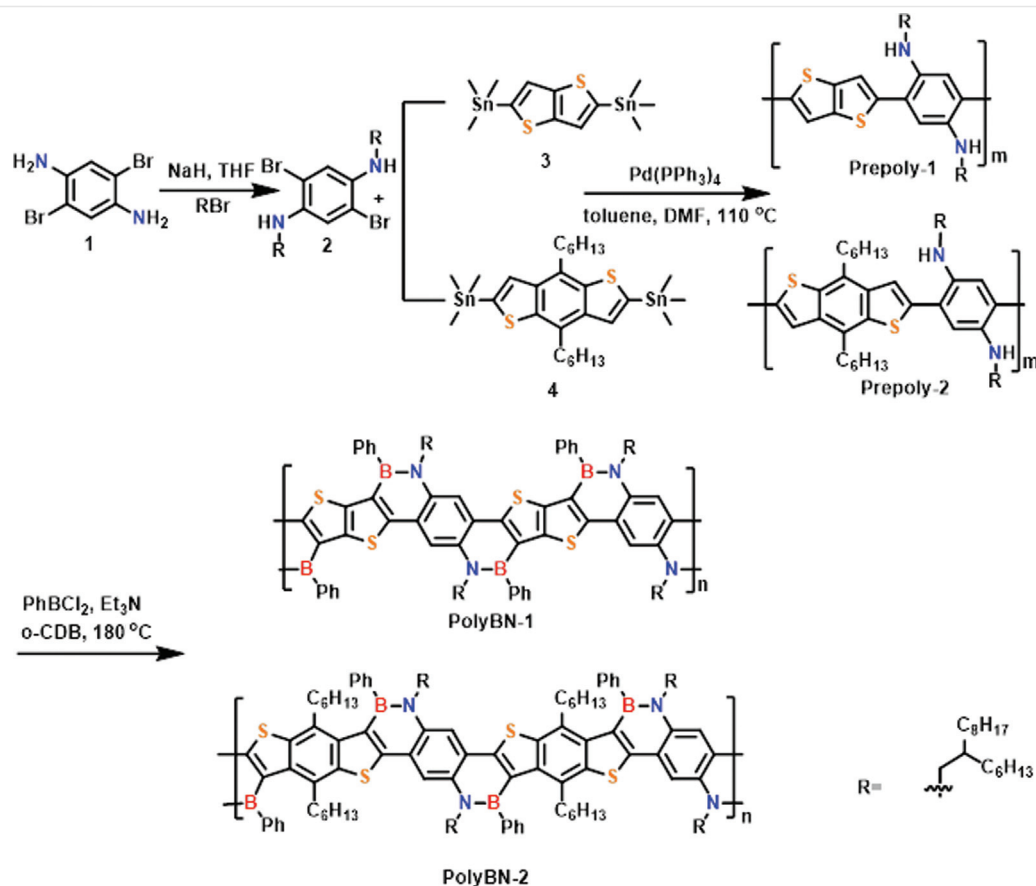
representing an efficient strategy for the direct carbon–hydrogen bond activation on aromatic rings, without the help of leaving groups.

In this work, we report a two-step approach to efficiently construct two kinds of ladder-type BN-annulated conjugated polymers. At first, the single-stranded conjugated polymers attached with amino groups were synthesized via transition-metal-catalyzed Stille cross-coupling reaction, which were further fused by nitrogen-directed electrophilic borylations at electron-rich aromatic rings. The resulting BN-annulated polymers were structurally characterized by NMR spectra and gel permeation chromatography (GPC) analyses. Their photophysical properties and electrochemical behaviors were also revealed by optical spectrum analyses and cyclic voltammetry (CV); combined with theoretical calculations, their electronic structures were rationally evaluated.

## Results and Discussion

The synthetic routes to the target cLPs **PolyBN-1** and **PolyBN-2** are depicted in Scheme 1. The key monomer 2,5-

dibromo-*N,N*-bis(2-hexyldecyl)benzene-1,4-diamine (**2**) was initially synthesized in 65% isolated yield, by attaching alky side chains to the amino groups of 2,5-dibromobenzene-1,4-diamine (**1**)<sup>47</sup> through typical nucleophilic substitution reaction. 2,5-Bis(trimethylstannyl)thieno[3,2-*b*] thiophene (**3**) and 1,1'-[4,8-dihexylbenzo [1,2-*b*:4,5-*b*'] dithiophene-2,6-diyl]bis[1,1,1-trimethylstannane] (**4**)<sup>48</sup> were achieved according to previous reports. Upon Pd-catalyzed Stille cross-coupling, monomer **2** was polymerized with the distannylated monomer **3** or **4** in a mixed solvent of toluene and DMF, resulting in the single-stranded conjugated polymer denoted as **Prepoly-1** or **Prepoly-2**, respectively. They were purified by Soxhlet extraction in different solvents with a sequence of methanol, acetone and hexane, for mainly removing off the low-molecular-weight fractions and catalyst residues, affording samples as dark red solid polymers in yields of 85% and 89%, respectively. Both of them showed excellent solubility in some common organic solvents, directly associated with the attached long alkyl chain on each of amino group, which is beneficial to their further modification or functionalization, meanwhile, declining the formation of structural defects. Such amino-



**Scheme 1** Synthetic routes to fully conjugated ladder-type polymers **PolyBN-1** and **PolyBN-2**.

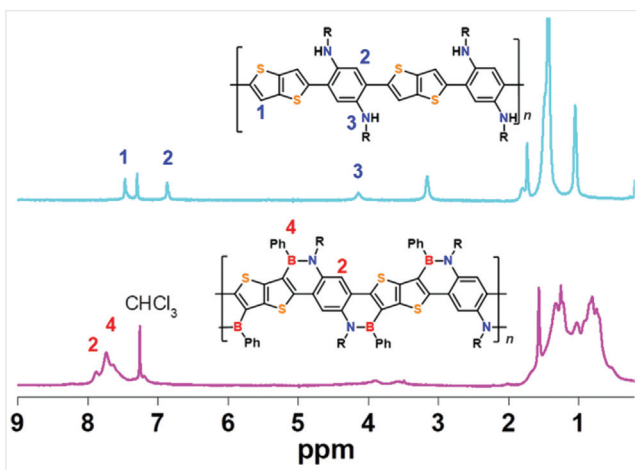


**Figure 2** <sup>1</sup>H NMR spectra of the **Prepoly-1** (top) and **PolyBN-1** (bottom) in  $\text{CDCl}_3$ .

substituted polymer **Prepoly-1** or **Prepoly-2** was employed with phenylboron dichloride in the presence of trimethylamine in *o*-dichlorobenzene, and heated up to 180 °C for a 12-h reaction. After removal of the solvent, the resultant residue was purified by precipitation in methanol for three times. The corresponding pure target polymer, termed **PolyBN-1** or **PolyBN-2**, was collected as red or orange powders, in yields of 95% and 94%, respectively. These two ladder polymers showed excellent stability without any obvious change when exposed to moisture or air for several weeks. The chemical structures of these new polymers were characterized by <sup>1</sup>H NMR spectra analysis. As an example, **Prepoly-1** showed two broad peaks at 7.44 and 6.82 ppm in the aromatic regions, attributed to protons 1 and 2, respectively (Figure 2). The peak at 4.05 ppm is arising from the amino protons. However, the peak at 3.03 ppm belongs to the protons of methylene directly connected to amino groups. The peaks between 0.87 and 1.63 ppm correspond to the other alkyl protons. As for **PolyBN-1**, the signals with respect to protons 1 and 3 in the profile of **Prepoly-1** disappeared, and a new peak was found at 7.89 ppm in the low field, likely originating from proton 2 of **PolyBN-1**. A broad peak from 7.40 to 7.81 ppm was assigned to the protons of phenyl groups attached on boron atoms. <sup>1</sup>H-NMR spectrum analyses of **PolyBN-1** at different temperatures (from 283 to 353 K) in toluene-*d*<sub>6</sub> were also performed. The resolutions of the characteristic signals in the aromatic regions somehow were improved at higher temperatures (Figure S8), indicating that the as-prepared ladder polymers tend to slightly aggregate at lower temperatures. The results clearly confirm that the single-stranded polymers bearing substantial amino groups have been efficiently achieved, which could be further smoothly converted to the ladder-type polymer **PolyBN-1** on the basis of amino-directed electrophilic borylation.

**Table 1** Molecular weight and thermal stability of **Prepoly-1**, **Prepoly-2**, **PolyBN-1** and **PolyBN-2**

Sample	$M_n/\text{kDa}$	PDI	$T_5\ (^{\circ}\text{C})$	$T_{10}\ (^{\circ}\text{C})$	$T_{50}\ (^{\circ}\text{C})$
<b>Prepoly-1</b>	–	–	350	363	409
<b>PolyBN-1</b>	10.69	1.46	380	427	480
<b>Prepoly-2</b>	–	–	370	385	422
<b>PolyBN-2</b>	9.41	1.40	382	423	480

Their molecular weights were measured by GPC, using THF as the eluent. The number-averaged molecular weights ( $M_n$ ) of the resulting polymers **PolyBN-1** and **PolyBN-2** were 10.69 and 9.41 kDa, with the polydispersity indices (PDIs) of 1.46 and 1.40, respectively (Table 1). Thermogravimetric analysis (TGA) of the polymers revealed their good thermal stability (Figure 3). The thermal degradation data of these polymers, including 5%, 10% and 50% mass-loss temperatures ( $T_5$ – $T_{50}$ ) are listed in Table 1. The decomposition temperatures ( $T_d$ , with 5% weight loss) of **Prepoly-1**, **Prepoly-2**, **PolyBN-1** and **PolyBN-2** were 350, 370, 380 and 382 °C, respectively. As expected, the thermal stability for the ladder-type polymers **PolyBN-1** and **PolyBN-2** is superior to those for **Prepoly-1** and **Prepoly-2**, further indicative of the highly rigid and fused skeletons in the former case.

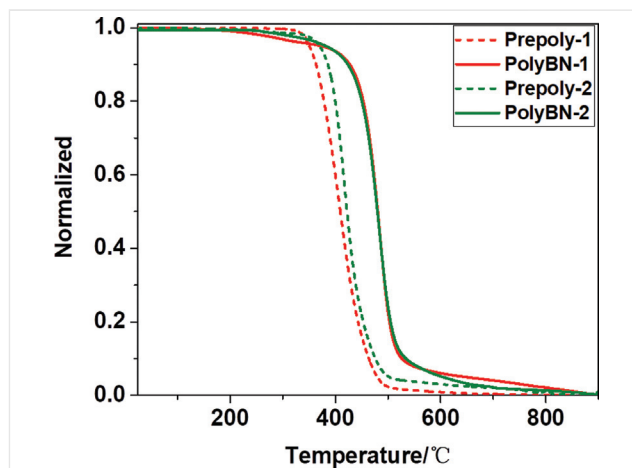


**Figure 3** TGA curves of the resulting polymers measured with a heating rate of 10 °C/min under flowing  $\text{N}_2$ .

The optical properties of these conjugated polymers were investigated by UV – vis and photoluminescence spectrum analyses. In absorption spectra (Figure 4a), **Prepoly-1** and **Prepoly-2** showed the broad absorption bands at 300–400 nm and 400–500 nm. The absorption bands in the UV regions were typically assigned to  $\pi$ – $\pi^*$  transitions of their

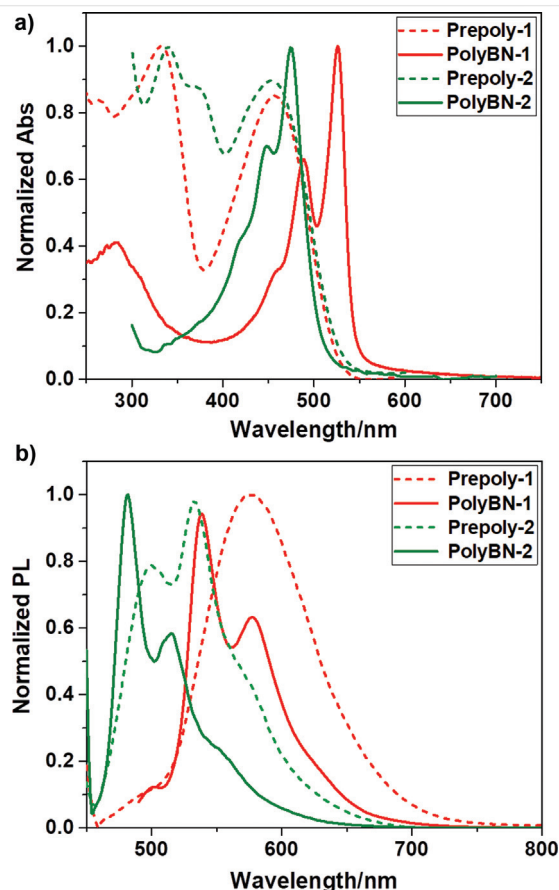


**Figure 4** a) Absorption and b) fluorescence spectra of **Prepoly-1**, **PolyBN-1** (red line) and **Prepoly-2**, **PolyBN-2** (green line) in DCM.

aromatic moieties. In the visible regions, the absorption maxima at 458 nm for **Prepoly-1** and at 454 nm for **Prepoly-2** are arising from the transitions of HOMO to LUMO energy levels. Such less-resolved broad peaks seem to reflect their low rigid main backbones rotatable around the single carbon–carbon bond linkages. However, the absorption maxima were observed at 526 nm for **PolyBN-1** and at 474 nm for **PolyBN-2**. In comparison to those of **Prepoly-1**

and **Prepoly-2**, well-resolved sharp absorption bands were observed, attributed to the restriction of the free rotation within highly rigid ladder-type structures in the case of **PolyBN-1** and **PolyBN-2**. Meanwhile, these absorption maxima appeared in much lower energy regions, indicating  $\pi$ -extended conjugated structures of such kinds of polymers. Notably, the absorption maxima for **PolyBN-1** were distinctly red-shifted as compared with those of **PolyBN-2**, which are consistent with the corresponding ladder-type small molecules **BN-1** and **BN-2** as shown in Figure 1. Such phenomenon was probably attributed to the declined planarity of the conjugated main backbone in the case of **PolyBN-2** according to the single crystal structures of ladder-type small molecules **BN-1** and **BN-2**. Different from the broad fluorescence emission bands of **Prepoly-1** and **Prepoly-2**, either **PolyBN-1** or **PolyBN-2** exhibited the narrowed and vibronically splitted fluorescence peaks. The emitting maxima of **PolyBN-1** and **PolyBN-2** were found at 538 and 481 nm, respectively. Accordingly, such two ladder-type polymers possess quite small Stokes shifts of 12 and 7 nm, respectively. Notably, such kinds of polymers can release strong yellow and green emission with the fluorescence quantum yields ( $\Phi_{PL}$ ) of 0.35 and 0.16, respectively, which are much higher than those of the ladder-type small molecules **BN-1** ( $\Phi_{PL}$ : 0.25) and **BN-2** ( $\Phi_{PL}$ : 0.02) (Table 2). And, their fluorescence profiles showed good mirror images of the corresponding absorption ones. These results considerably demonstrated the  $\pi$ -extended rigid planar structures of **PolyBN-1** and **PolyBN-2**. Additionally, their emission maxima showed obviously blue-shifted emission in comparison with **Prepoly-1** and **Prepoly-2**, suggesting the decreased exciton energy loss from non-radiative transitions, related to the restricted free rotation of main backbones for the ladder-type structures. No solvatochromic properties of **PolyBN-1** and **PolyBN-2** were observed in solvent-dependent measurements of absorption and fluorescence spectra, suggesting the lack of dipole moments in either the ground or the excited state for such kinds of ladder-type polymeric structures. In the films, the absorption and emission maxima of **PolyBN-1** and **PolyBN-2** show significant red-shifts, suggesting the strong intermolecular interactions (Figure S14).

**Table 2** Summary of the optical and electrochemical properties of the polymers

	UV – vis <sup>a</sup>		Fluorescence			Electrochemistry			Calculation	
	$\lambda_{max}$ (nm)	$E_g$ <sup>b</sup> (eV)	$\lambda_{max}$ (nm)	$\tau$ (ns)	$\Phi_{PL}$ <sup>c</sup>	$E_{HOMO}$ (eV) <sup>d</sup>	$E_{LUMO}$ (eV) <sup>e</sup>	$E_{ox}$ (V) <sup>f</sup>	HOMO (eV)	LUMO (eV)
<b>PolyBN-1</b>	526	1.88	538	2.7	0.35	-4.98	-3.10	0.18	-4.89	-1.49
<b>PolyBN-2</b>	474	2.01	481	1.6	0.16	-5.05	-2.95	0.25	-4.85	-1.46

<sup>a</sup>In DCM at 298 K.

<sup>b</sup> $E_g$ : optical band gap, estimated from UV – vis absorption edge.

<sup>c</sup>Absolute values.

<sup>d</sup>Calculated from the first oxidation peak using  $E_{HOMO} = -E_{ox} - 4.80$ .

<sup>e</sup>Calculated according to  $E_{LUMO} = E_{HOMO} + E_g$ .

<sup>f</sup>The first oxidation potential, estimated using the tangent method.

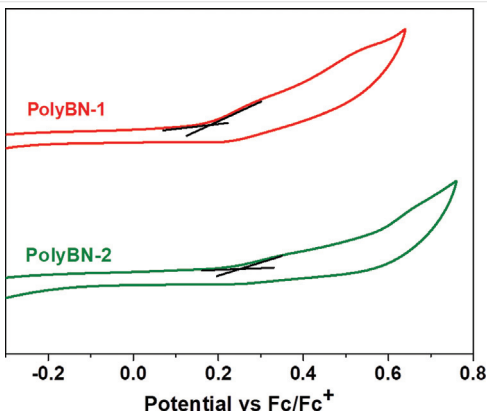


**Figure 5** Cyclic voltammogram of **PolyBN-1** and **PolyBN-2** measured in DCM (0.1 M  $n\text{-Bu}_4\text{NPF}_6$ ) at the scan rate of 0.1 V/s.

In order to get some insight into the electronic structures of these as-prepared polymers, their electrochemical behaviors were investigated through CVs in  $\text{CH}_2\text{Cl}_2$ . The CV profiles of **PolyBN-1** and **PolyBN-2** showed the irreversible oxidation processes under the measurement conditions, with the initial oxidation potentials at 0.18 V and 0.25 V, respectively (Figure 5), much lower than those of the ladder-type small molecules **BN-1** (0.59 V) and **BN-2** (0.66 V), indicative of the extended- $\pi$  conjugation for the as-prepared cLPs. Correspondingly, the HOMO energy levels of **PolyBN-1** ( $-4.98$  eV) and **PolyBN-2** ( $-5.05$  eV) and the LUMO energy levels of **PolyBN-1** (3.10 eV) and **PolyBN-2** (2.95 eV) were evaluated on the basis of their CV profiles and optical absorption edges (Table 2). The HOMO and LUMO energy levels of **PolyBN-1** and **PolyBN-2** significantly increased and decreased in comparison with those of the ladder-type small molecules **BN-1** and **BN-2**, respectively. The results clearly manifested the formation of the  $\pi$ -extended conjugated structures in a ladder-type polymeric backbone. However, **PolyBN-1** was easily oxidized compared with **PolyBN-2**, originated from the much electron-rich characters of the corresponding building block in the former one.

Eventually, electronic structures of these ladder-type polymers were investigated and evaluated on the basis of their elemental repeat structures, by density functional theory (DFT) calculations at the B3LYP/6-31G(d,p) level (Figure 6). DFT calculations demonstrated that HOMO and LUMO in these structures delocalized throughout the rigid coplanar backbones. The terminal rings showed slightly weaker aromatic character than those in the center. The phenyl groups attached in the molecular peripheries through boron atoms seem not contribute to both HOMO and LUMO. In the HOMO, the nitrogen and sulfur atoms have no significant contributions. In contrast, in the LUMO, all the atoms could provide contributions, but nitrogen showed slight contributions.

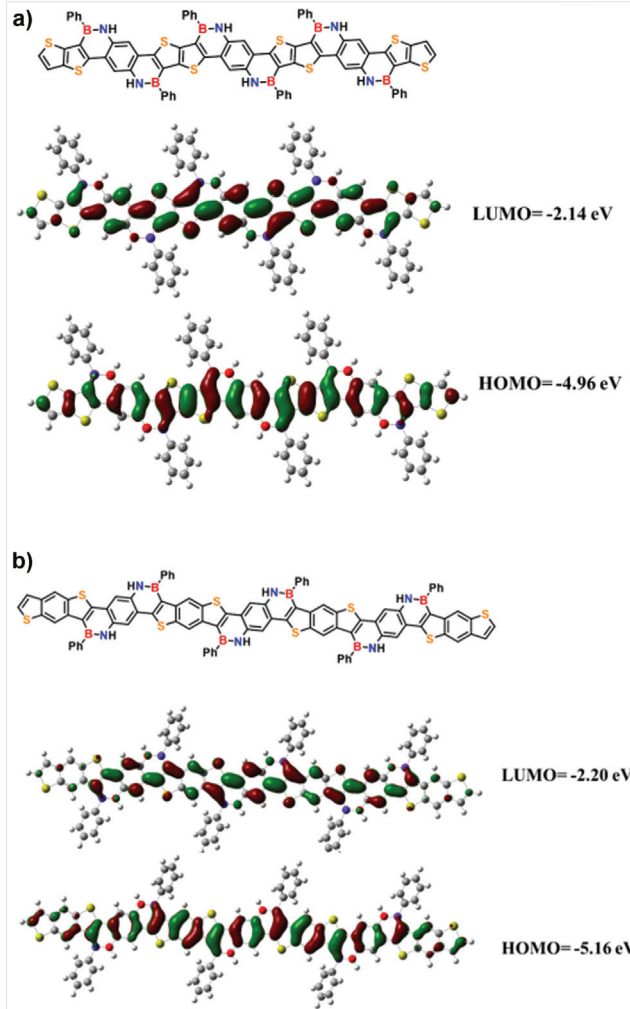


**Figure 6** HOMOs and LUMOs of **PolyBN-1** and **PolyBN-2**, calculated by DFT at the B3LYP/6-31G(d,p) level of theory (alkyl chains have been omitted for clarity).

## Conclusions

In conclusion, we have successfully synthesized two kinds of fully conjugated ladder BN-embedded polymers in high polymerization degrees, via the Stille cross-coupling reaction, followed by BN-annulation. These ladder-type conjugated polymers possess the  $\pi$ -extended shape-persistent rigid backbones, making them efficient for light harvesting in the low-energy regions, and releasing strong fluorescence with narrow emission bands. Generally, we have paved an efficient two-step approach to construct heteroatom-annulated conjugated structures for expanding the regimes of organic semiconducting materials. Combining their tunable electronic structures, good solubility in some common solvents and stable thermal stability, such kinds of polymers might be potentially applied in the fabrication of high-performance electronic devices.

## Experimental Section

All reagents were purchased from Sigma-Aldrich and Adamas-beta. Compound **1** was prepared using literature methods. All reactions were carried out under a nitrogen atmosphere and performed.

<sup>1</sup>H and <sup>13</sup>C NMR spectra were referenced to residual signals of the deuterated solvent. High-resolution electrospray ionization mass spectrometry was performed on a QToF spectrometer. UV-vis spectra were recorded on a HITACHI U-4100 spectrophotometer. The fluorescence spectroscopy emission spectra were obtained with a FluoroMax-4 spectrophotometer. CV was performed in anhydrous dichloromethane containing recrystallized tetra-*n*-butyl-ammonium hexafluorophosphate (TBAPF<sub>6</sub>; 0.1 M) as the supporting electrolyte at 298 K. A conventional three-electrode cell was used with a platinum working electrode (surface area of 0.3 mm<sup>2</sup>) and a platinum wire as the counter electrode. The Pt working electrode was routinely polished with a polishing alumina suspension and rinsed with acetone before use. The measured potentials were recorded with respect to the Ag/AgCl reference electrode. All electrochemical measurements were carried out under an atmospheric pressure of nitrogen. Geometry optimizations and the analysis of HOMOs and LUMOs were performed at the DFT level [RB3LYP/6-311G(d,p)].

## Procedures

### Synthesis of Compound 2

To a solution of 1,4-dibromo-2,5-diaminobenzene (**1**) (7.74 g, 29 mmol) in THF (210 mL) under nitrogen was added NaH (60% in oil, 3.85 g, 97 mmol) in small portions at 0 °C, and the mixed solution was stirred at room temperature for 30 min. The solution was refluxed for 2 h. After cooling to room temperature, 1-bromo-2-hexyldecane (15.88 g, 96 mmol) was added. The solution was refluxed for 13 h. The resulting mixture was cooled to room temperature and poured into water and extracted with ethyl acetate for several times. The organic phase was dried over MgSO<sub>4</sub> and the solvent was evaporated in vacuo. The product was purified by chromatography on silica gel to give the desired product as light yellow oil (6.5 g, 50%).

<sup>1</sup>H NMR (400 MHz, CDCl<sub>3</sub>, ppm): 7.38 (s, 1 H), 5.88 (s, 1 H), 4.15 (brs, 2 H), 3.11 (m, 4 H), 1.71–1.61 (m, 4 H), 1.47–1.30 (m, 12 H), 0.91 (m, 6 H).

<sup>13</sup>C NMR (100 MHz, CDCl<sub>3</sub>, ppm): 145.5, 134.3, 96.0, 94.2, 44.2, 31.8, 29.4, 27.0, 22.8, 14.3.

*m/z* [M + H]<sup>+</sup> calcd for C<sub>38</sub>H<sub>70</sub>Br<sub>2</sub>N<sub>2</sub>: 715.3964; HR-ESI observed: 715.3958

### Synthesis of Polymer (Prepoly-1)

A solution of compound **2** (142.6 mg, 0.2 mmol) and 5-bis(trimethylstannyl)thieno[3,2-*b*]thiophene (148.0 mg,

0.2 mmol) in 10 mL toluene and 10 mL DMF was degassed for 30 min. Afterwards, Pd(PPh<sub>3</sub>)<sub>4</sub> (1.8 mg) was added to the solution and then the mixture was heated to 110 °C and stirred for 72 h. The reactant was poured into methanol to get a solid. The solid was further purified by Soxhlet extraction sequentially in methanol, acetone, hexane, and then dissolved in chloroform. The solvent was removed under reduced pressure to get the target polymer **Prepoly-1** as red solid (117.8 mg, 85%).

<sup>1</sup>H NMR (400 MHz, CDCl<sub>3</sub>): δ 7.43 (br, 2 H), 6.82 (br, 2 H), 4.03 (br, 2 H), 3.02 (br, 4 H), 1.90–1.03 (br, 50 H), 0.86 (br, 12 H).

### Synthesis of Polymer (Prepoly-2)

A solution of compound **2** (142.6 mg, 0.2 mmol) and (4,8-dihexylbenzo[1,2-*b*:4,5-*b*']dithiophene-2,6-diyl)bis(trimethylstannane) (148.0 mg, 0.2 mmol) in 10 mL toluene and 10 mL DMF was degassed for 30 min. Afterwards, Pd(PPh<sub>3</sub>)<sub>4</sub> (1.8 mg) was added to the solution and then the mixture was heated to 110 °C and stirred for 72 h. The reactant was poured into methanol to get a solid. The solid was further purified by Soxhlet extraction sequentially in methanol, acetone, hexane, and then dissolved in chloroform. The solvent was removed under reduced pressure to get the target polymer **Prepoly-1** as red solid (184.2, 89%).

<sup>1</sup>H NMR (400 MHz, CDCl<sub>3</sub>): δ 7.67 (br, 2 H), 6.96 (br, 2 H), 4.17 (br, 2 H), 3.17 (br, 8 H), 2.17–1.01 (m, 66 H), 0.89 (m, 18 H).

### Synthesis of Polymer (PolyBN-1)

A mixture of **Prepoly-1** (150 mg, 0.17 mmol), phenylboron dichloride (1 M in DCM, 0.5 mL), triethylamine (400 mg, 4.0 mmol) and 1,2-dichlorobenzene (5 mL) was heated at reflux and stirred under nitrogen for 3 h. The solution was then cooled to room temperature, precipitated in methanol, and filtered. The solids were washed three times with methanol and petroleum ether. Then the residue was dried to yield **PolyBN-1** as a yellow solid (141.7 mg, 95%).

<sup>1</sup>H NMR (400 MHz, CDCl<sub>3</sub>): δ 7.88 (s, 2 H), 7.73 (s, 10 H), 4.12–3.39 (m, 6 H), 1.90–0.01 (m, 80 H).

<sup>11</sup>B NMR (160 MHz, CDCl<sub>3</sub>): δ ~30 ppm.

M<sub>n</sub> = 10.69 KDa, M<sub>w</sub>/M<sub>n</sub> = 1.46.

### Synthesis of Polymer (PolyBN-2)

A mixture of **Prepoly-2** (150 mg, 0.16 mmol), phenylboron dichloride (1 M in DCM, 0.5 mL), triethylamine (400 mg, 4.0 mmol) and 1,2-dichlorobenzene (5 mL) was heated at reflux and stirred under nitrogen for 3 h. The solution was then cooled to room temperature, precipitated in methanol, and filtered. The solids were washed three times with methanol and petroleum ether. Then the residue was dried to yield **PolyBN-2** as a yellow solid (143.3 mg, 94%).

<sup>1</sup>H NMR (400 MHz, CDCl<sub>3</sub>): δ 7.81 (br, 11 H), 3.70 (br, 10 H), 1.93–0.20 (br, 134 H).

M<sub>n</sub> = 9.41 KDa, M<sub>w</sub>/M<sub>n</sub> = 1.40.

<sup>11</sup>B NMR (160 MHz, CDCl<sub>3</sub>): undetected.

## Funding Information

We thank the National Natural Science Foundation of China (22075178), the Natural Science Foundation of Shanghai (20JC1414900), the China Postdoctoral Science Foundation (2020M681277), and the Fujian Engineering Research Center of New Chinese lacquer Material (Minjiang University) (No. 323030030702).

## Acknowledgment

We acknowledge the Instrumental Analysis Center of SJTU for the NMR, single crystal, and HRMS measurements.

## Supporting Information

Supporting information for this article is available online at <https://doi.org/10.1055/s-0041-1727181>.

## References

- (1) Lee, J.; Rajeeva, B. B.; Yuan, T. Y.; Guo, Z. H.; Lin, Y. H.; Al-Hashimi, M.; Zheng, Y. B.; Fang, L. *Chem. Sci.* **2016**, *7*, 881.
- (2) Zeng, S. Z.; Jin, N. Z.; Zhang, H. L.; Hai, B.; Chen, X. H.; Shi, J. L. *RSC Adv.* **2014**, *4*, 18676.
- (3) Wu, Y.; Zhang, J.; Fei, Z.; Bo, Z. *J. Am. Chem. Soc.* **2008**, *130*, 7192.
- (4) Teo, Y. C.; Lai, H. W. H.; Xia, Y. *Chem. Eur. J.* **2017**, *23*, 14101.
- (5) Lee, J.; Kalin, A. J.; Yuan, T. Y.; Al-Hashimi, M.; Fang, L. *Chem. Sci.* **2017**, *8*, 2503.
- (6) Chen, J. H.; Yang, K.; Zhou, X.; Guo, X. G. *Asian J. Org. Chem.* **2018**, *13*, 2587.
- (7) Grimsdale, A. C.; Mullen, K. *Macromol. Rapid Commun.* **2007**, *28*, 1676.
- (8) Scherf, U. *J. Mater. Chem. C* **1999**, *9*, 1853.
- (9) Samiullah, M.; Moghe, D.; Scherf, U.; Guha, S. *Phys. Rev. B: Condens. Matter* **2010**, *82*, 205211.
- (10) Prins, P.; Grozema, F. C.; Schins, J. M.; Patil, S.; Scherf, U.; Siebbeles, L. D. A. *Phys. Rev. Lett.* **2006**, *96*, 146601.
- (11) Grozema, F. C.; van Duijnen, P. T.; Berlin, Y. A.; Ratner, M. A.; Siebbeles, L. D. A. *J. Phys. Chem. B* **2002**, *106*, 7791.
- (12) Zenz, C.; Graupner, W.; Tasch, S.; Leising, G.; Mullen, K.; Scherf, U. *Appl. Phys. Lett.* **1997**, *71*, 2566.
- (13) Kallinger, C.; Hilmer, M.; Haugeneder, A.; Perner, M.; Spirk, W.; Lemmer, U.; Feldmann, J.; Scherf, U.; Mullen, K.; Gombert, A.; Wittwer, V. *Adv. Mater.* **1998**, *10*, 920.
- (14) Brisen, A. L.; Kim, F. S.; Babel, A.; Xia, Y. N.; Jenekhe, S. A. *J. Mater. Chem.* **2011**, *21*, 16461.
- (15) Brisen, A. L.; Mannsfeld, S. C. B.; Shamberger, P. J.; Ohuchi, F. S.; Bao, Z. N.; Jenekhe, S. A.; Xia, Y. N. *Chem. Mater.* **2008**, *20*, 4712.
- (16) Babel, A.; Jenekhe, S. A. *J. Am. Chem. Soc.* **2003**, *125*, 13656.
- (17) Chen, X. L.; Bao, Z. N.; Schon, J. H.; Lovinger, A. J.; Lin, Y. Y.; Crone, B.; Dodabalapur, A.; Batlogg, B. *Appl. Phys. Lett.* **2001**, *78*, 228.
- (18) Durban, M. M.; Kazarinoff, P. D.; Segawa, Y.; Luscombe, C. K. *Macromolecules* **2011**, *44*, 4721.
- (19) Piok, T.; Gamerith, S.; Gadermaier, C.; Plank, H.; Wenzl, F. P.; Patil, S.; Montenegro, R.; Kietzke, T.; Neher, D.; Scherf, U.; Landfester, K.; List, E. *J. W. Adv. Mater.* **2003**, *15*, 800.
- (20) Crossley, D. L.; Cade, I. A.; Clark, E. R.; Escande, A.; Humphries, M. J.; King, S. M.; Vitorica-Yrezabal, I.; Ingleson, M. J.; Turner, M. L. *Chem. Sci.* **2015**, *6*, 5144.
- (21) Zhu, C.; Guo, Z. H.; Mu, A. U.; Liu, Y.; Wheeler, S. E.; Fang, L. *J. Org. Chem.* **2016**, *81*, 4347.
- (22) Tian, Y. H.; Kertesz, M. *Macromolecules* **2009**, *42*, 2309.
- (23) Wakamiya, A.; Taniguchi, T.; Yamaguchi, S. *Angew. Chem. Int. Ed.* **2006**, *45*, 3170.
- (24) Vetrichelvan, M.; Valiyaveettill, S. *Chem. Eur. J.* **2005**, *11*, 5889.
- (25) Schluter, A. D.; Loffler, M.; Enkelmann, V. *Nature* **1994**, *368*, 831.
- (26) Zou, Y.; Ji, X. Z.; Cai, J. Z.; Yuan, T. Y.; Stanton, D. J.; Lin, Y. H.; Naraghi, M.; Fang, L. *Chem* **2017**, *2*, 139.
- (27) Cho, S. Y.; Grimsdale, A. C.; Jones, D. J.; Watkins, S. E.; Holmes, A. B. *J. Am. Chem. Soc.* **2007**, *129*, 11910.
- (28) Patil, S. A.; Scherf, U.; Kadashchuk, A. *Adv. Funct. Mater.* **2003**, *13*, 609.
- (29) Nehls, B. S.; Fuldrer, S.; Preis, E.; Farrell, T.; Scherf, U. *Macromolecules* **2005**, *38*, 687.
- (30) Kass, K. J.; Forster, M.; Scherf, U. *Angew. Chem. Int. Ed.* **2016**, *55*, 7816.
- (31) Yuan, Z. Y.; Xiao, Y.; Yang, Y.; Xiong, T. *Macromolecules* **2011**, *44*, 1788.
- (32) Daigle, M.; Miao, D.; Lucotti, A.; Tommasini, M.; Morin, J. F. *Angew. Chem. Int. Ed.* **2017**, *56*, 6213.
- (33) Chalifoux, W. A. *Angew. Chem. Int. Ed.* **2017**, *56*, 8048.
- (34) Bheemireddy, S. R.; Hautzinger, M. P.; Li, T.; Lee, B.; Plunkett, K. N. *J. Am. Chem. Soc.* **2017**, *139*, 5801.
- (35) Liu, J.; Li, B. W.; Tan, Y. Z.; Giannakopoulos, A.; Sanchez-Sanchez, C.; Beljon, D.; Ruffieux, P.; Fasel, R.; Feng, X.; Müllen, K. *J. Am. Chem. Soc.* **2015**, *137*, 6097.
- (36) Wang, X. Y.; Lin, H. R.; Lei, T.; Yang, D. C.; Zhuang, F. D.; Wang, J. Y.; Yuan, S. C.; Pei, J. *Angew. Chem. Int. Ed.* **2013**, *52*, 3117.
- (37) Wang, X.; Zhang, F.; Liu, J.; Tang, R.; Fu, Y.; Wu, D.; Xu, Q.; Zhuang, X.; He, G.; Feng, X. *Org. Lett.* **2013**, *15*, 5714.
- (38) Li, G.; Xiong, W. W.; Gu, P. Y.; Cao, J.; Zhu, J.; Ganguly, R.; Li, Y.; Grimsdale, A. C.; Zhang, Q. *Org. Lett.* **2015**, *17*, 560.
- (39) Wang, X.; Zhang, F.; Gao, J.; Fu, Y.; Zhao, W.; Tang, R.; Zhang, W.; Zhuang, X.; Feng, X. *J. Org. Chem.* **2015**, *80*, 10127.
- (40) Zhou, J.; Tang, R. Z.; Wang, X. Y.; Zhang, W. Z.; Zhuang, X. D.; Zhang, F. *J. Mater. Chem. C* **2016**, *4*, 1159.
- (41) Zhang, W.; Zhang, F.; Tang, R.; Fu, Y.; Wang, X.; Zhuang, X.; He, G.; Feng, X. *Org. Lett.* **2016**, *18*, 3618.
- (42) Matsui, K.; Oda, S.; Yoshiura, K.; Nakajima, K.; Yasuda, N.; Hatakeyama, T. *J. Am. Chem. Soc.* **2018**, *140*, 1195.
- (43) Li, G.; Zhao, Y.; Li, J.; Cao, J.; Zhu, J.; Sun, X. W.; Zhang, Q. *J. Org. Chem.* **2015**, *80*, 196.
- (44) Yao, C. J.; Zhao, K. X.; Long, G.; Li, X. K.; Gong, Z. L.; Zhong, Y. W.; Gao, W. B.; Li, Y. X.; Ganguly, R.; Li, G.; Zhang, Q. *C. New J. Chem.* **2019**, *43*, 564.
- (45) Zhao, R.; Liu, J.; Wang, L. *Acc. Chem. Res.* **2020**, *53*, 1557.
- (46) Zhao, R. Y.; Wang, N.; Yu, Y. J.; Liu, J. *Chem. Mater.* **2020**, *32*, 1308.
- (47) Nakamura, T.; Furukawa, S.; Nakamura, E. *Chem. Asian J.* **2016**, *11*, 2016.
- (48) Liang, Y.; Feng, D.; Wu, Y.; Tsai, S. T.; Li, G.; Ray, C.; Yu, L. *J. Am. Chem. Soc.* **2009**, *131*, 7792.